JTTEE5 17:812–817
DOI: 10.1007/s11666-008-9253-6
1059-9630/$19.00 © ASM International

HVOF-Sprayed Nylon-11 + Nanodiamond Composite Coatings: Production & Characterization

A. Stravato, R. Knight, V. Mochalin, and S.C. Picardi

(Submitted July 2, 2008; in revised form August 22, 2008)

High velocity oxy-fuel (HVOF) combustion spraying has previously been shown to be a viable method for depositing polymer and polymer/ceramic composite coatings. The addition of hard particulate reinforcing phases to soft polymeric matrices should improve their durability and sliding wear performance. Nanosized diamond is an ideal reinforcing phase, owing to its high hardness, low coefficient of friction, and desirable thermal properties. Composite coatings comprising a Nylon-11 matrix reinforced with nanodiamonds have been successfully produced by HVOF. An important challenge is preserving the structure of the nanoparticles after thermal spray deposition and achieving their uniform dispersion within the polymeric matrix. Raman spectroscopy and x-ray diffraction were used to confirm the presence and retention of nanodiamonds after HVOF deposition. Understanding of the role of process parameters, including the content of reinforcing phase in the matrix and powder preparation route is necessary. Nanoindentation studies demonstrated an improvement in creep behavior and recovery of the HVOF Nylon-11/nanodiamond composites subjected to deformation.

Keywords functionalization, HVOF spraying of polymers, nanocomposites, nanodiamonds

1. Introduction

Nanoreinforced polymer composites have attracted increased attention because they exhibit unique properties compared to their conventional microreinforced counterparts. Ultradispersed (UDD) or nanocrystalline diamond, often referred to as ''nanodiamond'' (ND), is an ideal and desirable reinforcing phase due to its nanometer size and unique properties of diamond such as extreme hardness, high Young's modulus, high electrical resistivity, and high thermal conductivity. ND powder is produced at high pressure under nonequilibrium conditions by detonation synthesis from carbon-containing explosives with negative oxygen balance such as a mixture of TNT and RDX (Ref 1). Several applications of ND have recently been explored, including the deposition of wear- and corrosion-resistant metal coatings, additives to cooling fluids, lubricants, and polishing compositions for ultraflat optical or magnetic components (Ref 2, 3).

A key technical challenge in processing these composites is achieving a uniform dispersion and distribution of the nanofiller within the polymer matrix. Another challenge is to improve the interfacial bonding between the nanodiamond particles and polymer matrix. Previous results (Ref 4-6) demonstrated that the high velocity oxy-fuel (HVOF) combustion spray technique can be used to deposit polymers and polymer matrix nanocomposites incorporating ceramic phases such as silica and alumina without any need for volatile solvents. The size and morphology of the nanoparticles strongly affect their rate of heating and acceleration and, hence, the efficiency of deposition as well as structure and properties of the coating. Nanosized powders tend to agglomerate and can easily obstruct the feeding system, adhere to the walls of the nozzle, and be lost during spraying, resulting in a loss of material, and hence money. To avoid these problems, appropriate attention must be paid to preparation of the feedstock powders and optimization of the spraying parameters.

This paper reports on the first successful HVOF deposition of Nylon-11/nanodiamond composite coatings, preserving the structure of the nanodiamonds in the deposit microstructure. Nylon 11 was chosen because of its industrial significance and potential use in the powder coating industry. It is also one of the very few synthetic polymers produced from a natural source—the precursor for Nylon-11 is 11-aminoundecanoic acid monomer, typically manufactured from castor oil.

This article is an invited paper selected from presentations at the 2008 International Thermal Spray Conference and has been expanded from the original presentation. It is simultaneously published in *Thermal Spray Crossing Borders, Proceedings of the 2008 International Thermal Spray Conference*, Maastricht, The Netherlands, June 2-4, 2008, Basil R. Marple, Margaret M. Hyland, Yuk-Chiu Lau, Chang-Jiu Li, Rogerio S. Lima, and Ghislain Montavon, Ed., ASM International, Materials Park, OH, 2008.

A. Stravato, Dipartimento Ingegneria Meccanica e Industriale, Università degli Studi ''Roma Tre'', via della Vasca Navale 79, 00146, Rome, , Italy; **R. Knight** and **V. Mochalin**, Department of Materials Science and Engineering, Drexel University, 3141 Chestnut Street, Philadelphia, PA; and **S.C. Picardi**, Nanoblox, Inc., Boca Raton, FL. Contact e-mail: knightr@coe.drexel.edu.

2. Experimental Approach

2.1 Materials Selection

Semicrystalline Nylon-11 (Polyamide-11) powder, available commercially as Rilsan® D, ''French Natural ES'' (donated by Arkema, Inc., King of Prussia, PA) with nominal 80 μm particle size (designated D80), was selected as the feedstock for the experiments.

Nanodiamond (ND) powder (UD90 grade) produced by detonation synthesis was supplied by NanoBlox, Inc., (Boca Raton, FL). The as-produced powder was thoroughly characterized previously (Ref 7) using Raman spectroscopy, TEM, XANES, and FTIR. The ND particles have a diamond sp^3 core, covered by diverse functional groups such as -COOH, -OH, hydrocarbon chains, and surrounded by amorphous and graphitic carbon shells incorporating metal impurities. The as-produced UD90 was purified by the manufacturer through a multistage acid treatment with nitric and sulfuric acids. Additional oxidative purification in air at 425 °C was used to selectively remove the non-diamond carbon phases around the diamond cores of the nanoparticles (Ref 7). Air oxidation was followed by a treatment with boiling aqueous HCl to remove metal impurities, which become accessible after the oxidation of amorphous and graphitic carbon. This treatment, while removing metals and metal oxides from the surface, increases the number of surface carboxylic groups. IR spectra of as-received and purified ND (Fig. 1) reveal an increased number of oxygen-containing COOH, $=(CO)_2O$ (anhydro-), and OH groups. The higher content of ionogenic oxygen-containing surface functional groups results in a better aqueous dispersion stability of the oxidized HCl-treated nanodiamond as compared to as-received and oxidized nanodiamond at pH 7-9.

2.2 Feedstock Powder Preparation

Nylon-11 powder was dry ball-milled together with as-received UD90 nanodiamond powder for 48 h in a Norton Ball Mill using zirconia balls. The milling procedure mechanically embedded the hard reinforcement particles into the surface of the Nylon-11 powder particles. Composite powders with 2.5 to 10 vol.% (7 to 25 wt.%) nanodiamond loadings were produced for subsequent HVOF spray consolidation, as described below.

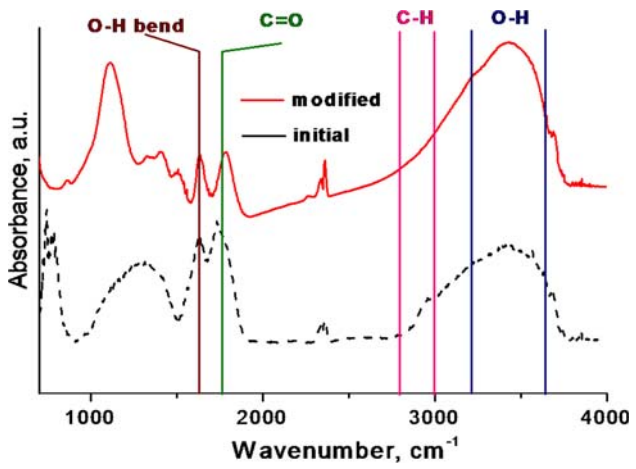

Fig. 1 IR spectra of UD90 powder before and after the air oxidation and HCl treatment

2.3 Thermal Spray Experiments

Spraying of the composite feedstock powders was carried out using a Jet Kote II® HVOF combustion spray system (Deloro Stellite, Inc., Goshen, IN) at oxygen and hydrogen flow rates of 0.0024 and 0.0039 m^3/s (300 and 500 scfh), respectively, and a spray distance of 200 mm (8 in.). Powders were fed using a Praxair Model 1207 volumetric powder feeder (Praxair Surface Technologies, Inc., Indianapolis, IN) with nitrogen as a powder carrier gas at a flow rate of 0.5×10^{-4} m^3 s^{-1} (60 scfh). A 76 mm long by 6 mm ID (3 × ¼ in.) spray nozzle was used. The materials were deposited using a gun traverse speed of ~0.06 m s^{-1}, with external compressed air substrate cooling (410 kPa or 60 psi) with a 6 mm step size between passes. Coatings were deposited onto steel substrates, grit blasted prior to spraying using 50-mesh angular alumina grit from a Trinco model 24/BP2 (Fraser, MI) grit blast cabinet. The substrates were preheated with the HVOF jet to ~180 °C before spraying.

2.4 Coating Characterization

Cross-sectional samples of the sprayed coatings were prepared using standard metallographic techniques: sectioning, mounting, and polishing with 400 and 600 grit SiC papers and 5 μm alumina powder.

Raman spectra were recorded using a Renishaw Model 1000 spectrometer (Renishaw, UK) with an excitation wavelength of 325 nm (He-Cd laser) in a backscatter configuration. Each Raman spectrum was obtained as an average of three accumulations recorded from three different spots on the sample with 300 s accumulation time. To minimize the thermal destruction of the samples caused by the UV laser, the samples were immersed in deionized water during exposure to the laser. Spectra were analyzed using the Renishaw *Wire 2.0* software.

X-ray diffraction (XRD) analysis was performed using a Siemens D500 x-ray powder diffractometer (Bruker AXS, Inc., Madison, WI) (Cu Kα, $\lambda = 1.54056$ Å) with a step size of 0.02° (2θ) and a hold time of 1 s. Results were analyzed using the MDI Jade 7 analysis software (Materials Data, Inc., Livermore, CA). Samples for XRD analysis were sprayed on glass substrates, rather than steel, to eliminate x-ray peaks from the steel determined to be close to the expected peaks of diamond.

Room temperature mechanical properties of the sprayed polymer/nanodiamond deposits were studied by nanoindentation using a Nanoindenter XP system (MTS Corp., Oak Ridge, TN) equipped with a continuous stiffness measurement (CSM) attachment. Each sample cross section was indented 10 times using a conical indenter with a 13.5 μm radius spherical tip, at 4000 nm maximum indentation depth with an allowable drift rate of 0.1 nm/s.

Using the Oliver and Pharr model (Ref 8), the contact depth h_c and hence the contact radius a were determined according to the following equations:

$$h_c = h - \varepsilon \cdot (P/S)$$

$$a = \sqrt{2h_c R - h_c^2}$$

where h is the total displacement, S the contact stiffness measured by the CSM, and ε a geometric constant that is 0.75 for a spherical indenter. From Hertz's theory E_r can be calculated as

$$E_r = \frac{\sqrt{\pi \cdot S}}{2\sqrt{A}}$$

where E_r is the reduced modulus, E_r is also given by

$$E_r = \frac{1 - \nu_i^2}{E_i} + \frac{1 - \nu_s^2}{E_s}$$

where i and s refer to the indenter and specimen, respectively.

The hardness H is defined as the indentation load divided by the projected contact area $A = \pi a^2$

$$H = P/A$$

Further details can be found in Ref 8.

3. Results and Discussion

X-ray diffraction (XRD) and Raman spectroscopy were used to confirm the retention and presence of nanodiamonds in the coatings after HVOF spraying. XRD patterns of a 13 wt.% ND-Nylon-11 coating sprayed onto glass are shown in Fig. 2. The peaks at 20.5 and 23.5° are related to the polymer. Curve b (red) shows the XRD diffraction pattern of the nanocrystalline diamond powder (Ref 9, 10). The peaks of ND were present in the XRD spectra of the coating (curve a, blue) confirming the presence of diamond in the deposited coating.

Additional confirmation of the presence of nanodiamonds in the HVOF-sprayed coatings was obtained via UV Raman spectroscopy. The UV Raman spectrum of a typical ND powder exhibits the G band of sp^2 carbon at ~1610 cm^{-1} originating from amorphous carbon, carbon onions, and fullerene-like shells, the disorder-induced double-resonance D band around 1400 cm^{-1}, and the diamond peak at ~1325 cm^{-1} that is downshifted compared to the normal bulk diamond peak at 1332 cm^{-1} (Ref 7, 11). In Fig. 2 the D band is weak and not seen. The Raman spectrum of Nylon-11 overlaps with the spectrum of ND (curve *a* in Fig. 3); moreover, the polymer shows high fluorescence level under UV laser excitation. Therefore, to eliminate the contribution of polymer, the coating was dissolved in a 1:1 (by volume) mixture of formic acid and dichloromethane (Ref 12). The Raman spectra were collected after rinsing the resulting powder several times with fresh solvent (Fig. 3b). The peak at

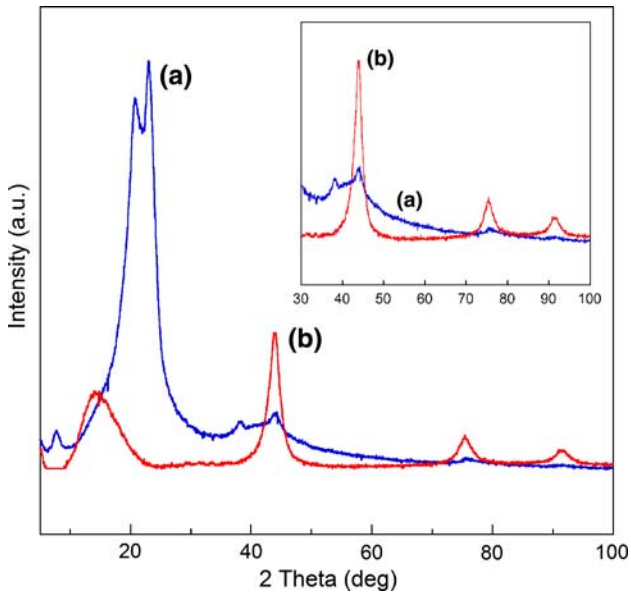

Fig. 2 X-ray spectra of (a) Nylon-11/nanodiamond coating and (b) nanodiamond powder. The inset region shows an enlargement of the three primary peaks of nanodiamond

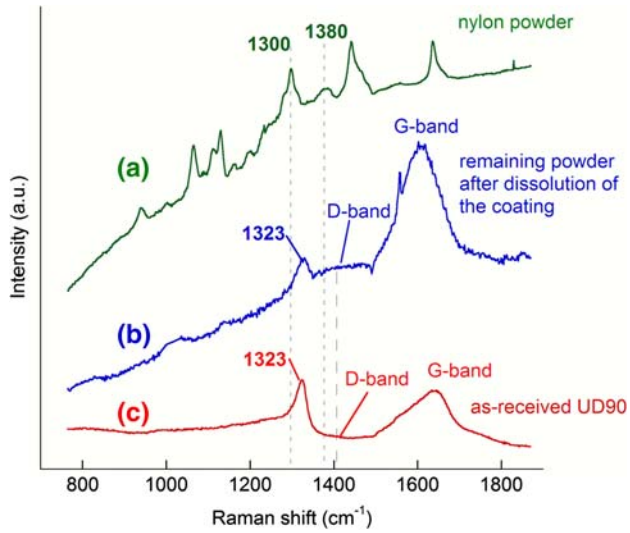

Fig. 3 Raman spectra of coating on a glass substrate (a); powder collected after the dissolution of the polymer in the coating (b); and ND powder (c)

1325 cm^{-1} shown in Fig. 3(b), observed after the polymer dissolution, was assigned to the ND, thus confirming the presence of the diamond phase in the sprayed coating. The low intensity of the G-band (~1600 cm^{-1}) in Fig. 2(b) led to the conclusion that the HVOF process did not result in any significant graphitization of the nanodiamond.

Figure 4 shows the typical loading-hold-unloading nanoindentation curves for coatings with different nanodiamond contents. When the load is released from the indenter, the material attempts to regain its original shape,

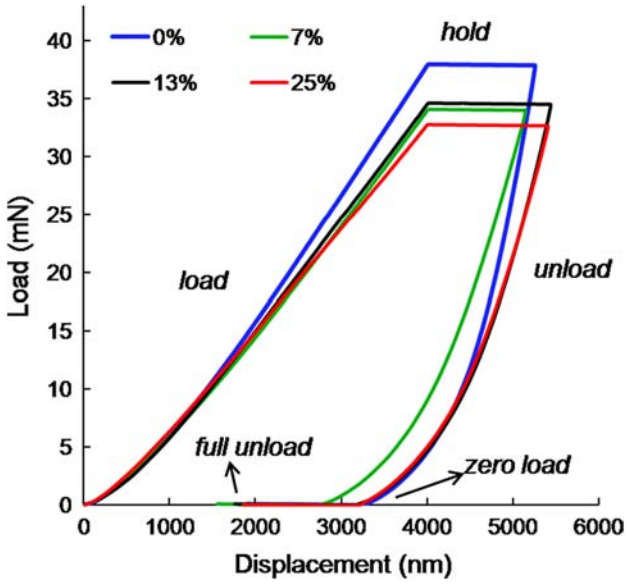

Fig. 4 Loading-hold-displacement curves for HVOF-sprayed Nylon-11/nanodiamond coatings with varying nanodiamond content

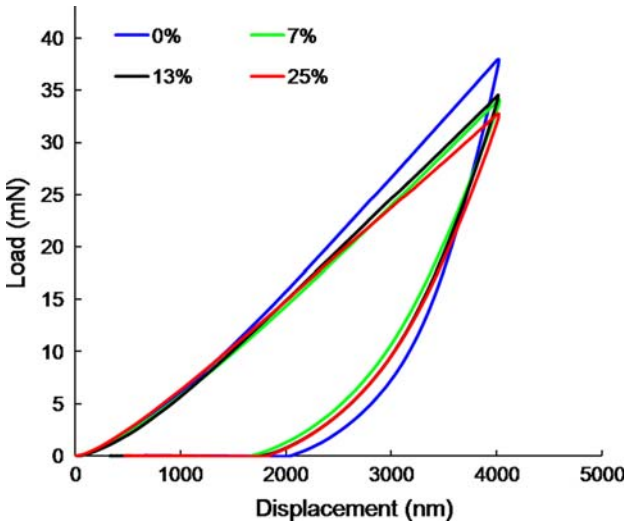

Fig. 5 Load-displacement curves for HVOF-sprayed Nylon-11/nanodiamond coatings with varying nanodiamond content

but usually the recovery is not 100%, indicating a level of plastic deformation. After the complete removal of the load, the material slowly continued to recover the original shape with a delay due to the relaxation of the polymer chains, giving origin to different recovery values at zero load (removal of the load) and at full unloading (complete relaxation of the elastic strain in the material). To better visualize this recovery behavior, Fig. 5 shows the indentation curves for the coatings without the holding segment. The recovery at zero load and the recovery at full unloading are reported in Table 1. The data are the mean of 10 indents for each sample and are presented as a percentage of the total depth (Recovery * 100/total depth).

The presence of nanodiamond is expected to influence the viscoelastic behavior of the polymer. The nanoparticles in the matrix limit the mobility of the polymer chains and conformation changes. The chains are confined at nanoscale. The presence of nanodiamonds reduces the dissipation of energy during the deformation process so that the coatings with higher nanodiamond contents tend to return more energy at the end of the unloading cycle. This resulted in a slight trend of decrease of the residual depth compared to that for the pure polymer. Thus, the mean values of recovery at zero load and recovery at full unload are systematically higher for samples with nanodiamond as compared to the neat polymer (Table 1). The large values of standard deviations for both these parameters are due to the surface roughness and common problems with precise definition of the sample surface in nanoindentation.

The length of the creep zone at the maximum load divided by time (the average creep rate) is reported in Table 1. There was a slight decrease in the creep rate for the sample with 7 wt.% of ND. The hardness and

Table 1 Elastic recovery and average creep rate of the coatings

Nanodiamond loading, wt.%	Recovery at zero load, %	Recovery at full unload, %	Average creep rate, nm/s
0	49 ± 4	82 ± 5	1.21 ± 0.03
7	56 ± 12	88 ± 7	1.12 ± 0.03
13	56 ± 14	93 ± 4	1.41 ± 0.03
25	50 ± 22	87 ± 8	1.32 ± 0.04

modulus, calculated from the continuous stiffness measurement (CSM), are reported in Fig. 6. Overall, the improvement in the mechanical properties of the composites, measured by nanoindentation, was not as significant as expected. One of the reasons may be a poor distribution/dispersion of the nanodiamonds in the final coatings. This is a well-known common issue in the realization of the nanocomposites (Ref 13) and still is to be addressed.

Another key property of sprayed coatings is their adhesion to the substrate. For the HVOF coatings produced in this work, their adhesion to the substrate was significantly improved upon addition of the nanodiamond. Figure 7 compares optical images of a coating with 7 wt.% of nanodiamond and a pure Nylon-11 coating sprayed using the same parameters. Small regions of the coatings were peeled off using a razor blade. The sprayed pure Nylon-11 coating was readily peeled off whereas the Nylon-11/nanodiamond composite coating could not be peeled off at all without scratching the underlying metallic substrate, indicating significantly improved adhesion in the latter case.

It is known that many properties of nanoparticles are determined by their surface chemistry (Ref 14). The surface of the nanoparticles governs their dispersion/agglomeration behavior in solvents, interaction with the environment, biocompatibility, etc. Therefore, the full control and manipulation of the surface chemistry is

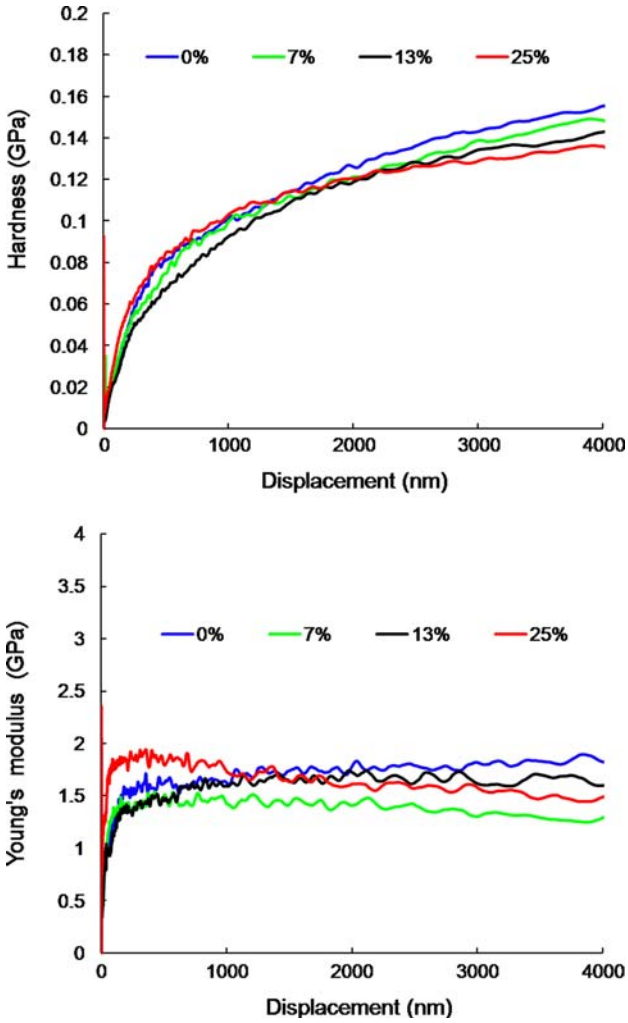

Fig. 6 Hardness (upper) and elastic modulus (lower) versus displacement for HVOF-sprayed Nylon-11/nanodiamond coatings with varying loadings of nanodiamond

important for optimal design of nanodiamond-polymer composites. Having the ability to purify the nanodiamond and control its surface chemistry allowed conversion of the majority of the surface functionalities to -COOH groups (Ref 7). Subsequent treatment with a dilute aqueous HCl, which is a standard step to remove metal impurities, increases the content of surface carboxylic groups through conversion of anhydrides into COOH. Carboxyl groups at the surface of ND are believed to interact with the nitrogen and oxygen atoms of the amide groups in the backbone of the Nylon-11 chain through the formation of hydrogen bonds. The formation of hydrogen bonds results in stronger interactions between the polymer and nanodiamond particles and more uniform distribution of the particles within the polymer matrix.

Scanning electron microscopy images of the surface of the polymer covered with oxidized HCl-treated UD90 (9 wt.% of ND) and as-received UD90 (13 wt.% of ND) are shown in Fig. 8. Despite the lower content of nanodiamonds, the oxidized HCl-treated UD90 shows a better coverage of the surface and a higher level of deagglomeration compared to the as-received one. Therefore, it is believed that substitution of the as-received UD90 with the oxidized and HCl treated UD90 will result in further improvement in properties of HVOF ND-containing Nylon-11 coatings.

4. Summary and Conclusions

This work has demonstrated the feasibility of producing polymer matrix nanocomposites incorporating nanodiamond as the reinforcing phase via thermal spray. X-ray diffraction and Raman spectroscopy confirmed the presence of nanodiamonds in the sprayed deposits. Qualitative assessment indicated that coating adhesion was improved through the addition of the nanodiamond to the Nylon-11.

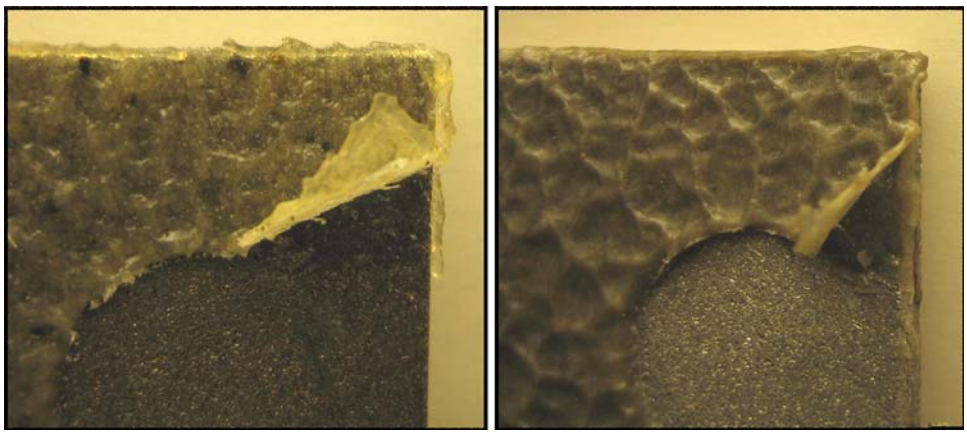

Fig. 7 Optical images of HVOF-sprayed (L) pure Nylon-11 coating and (R) Nylon-11 with 7 wt.% nanodiamond

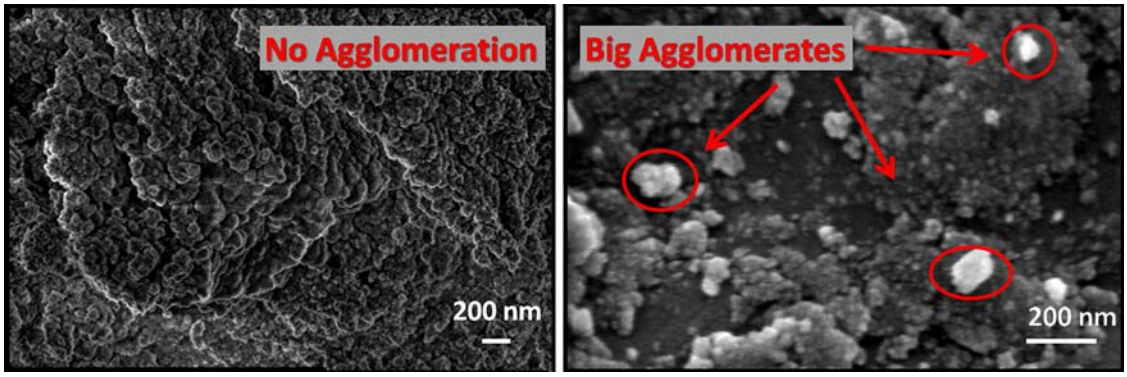

Fig. 8 SEM image of the surface of Nylon-11 covered by oxidized and HCl-treated UD90 (L) and by UD90 (R) as-received

Feedstock preparation is an important aspect and further work is clearly needed to investigate and optimize the process for better dispersion and covalent bonding of the nanodiamond particles to the polymer matrix and for characterizing the improvement in properties as a function of nanodiamond content.

These results indicate significant promise for the HVOF-produced nanodiamond-polymer composites and should lead to future applications for these materials. Nanodiamonds may also be used in place of, or in addition to, more conventional reinforcing phases, such as WC or Cr_3C_2, where their extreme hardness, low coefficient of friction, high thermal conductivity, and modest cost (~$1 per gram) may enable more environmentally friendly and improved wear resistant coatings to be developed.

Acknowledgments

The authors would like to acknowledge NanoBlox®, Inc. for supplying the nanodiamond powders and Arkema, Inc. for donating the Nylon-11 powders used in this work. The authors are grateful for the assistance of Mr. Dustin Doss, Ms. Dee Breger, Dr. Zhorro Nikolov, and the Centralized Research Facilities (CRF) at Drexel University. The authors would also like to thank K. Behler and S. Picchiotti for the helpful discussions.

References

1. V.V. Danilenko, Specific Features of Synthesis of Detonation Nanodiamonds, *Combust. Explo. Shock Waves*, 2005, **41**(5), p 577-588
2. G. Post, V.Y. Dolmatov, V.A. Marchukov, V.G. Sushchev, M.V. Veretennikova, and A.E. Sal'ko, Industrial Synthesis of Ultradisperse Detonation Diamonds and Some Fields of Their Use, *Russ. J. Appl. Chem.*, 2002, **75**(5), p 755-760
3. V. Livramento, J.B. Correia, N. Shohoji, and E. Ōsawa, Nanodiamond as an Effective Reinforcing Component for Nano-Copper, *Diam. Relat. Mater.*, 2007, **16**, p 202-204
4. E. Petrovicova, R. Knight, L.S. Schadler, and T.E. Twardowski, Nylon-11/Silica Nanocomposite Coatings Applied by the HVOF Process I. Microstructure and Morphology, *J. Appl. Polym. Sci.*, 2000, **77**, p 1684-1699
5. E. Petrovicova, R. Knight, L.S. Schadler, and T.E. Twardowski, Nylon-11/Silica Nanocomposite Coatings Applied by the HVOF Process II. Mechanical and Barrier Properties, *J. Appl. Polym. Sci.*, 2000, **78**, p 2272-2289
6. N. Ivosevic, R.A. Cairncross, and R. Knight, Melting and Degradation of Nylon-11 Particles during HVOF Combustion Spraying, *Proceedings of the 2007 International Thermal Spray Conference*, (ITSC-2007), (Beijing), ASM International, 2007, p 820-825
7. S. Osswald, et al., Control of sp^2/sp^3 Carbon Ratio and Surface Chemistry of Nanodiamond Powders by Selective Oxidation in Air, *J. Am. Chem. Soc.*, 2006, **128**(35), p 11635-11642
8. A.C. Fischer-Cripps, A Review of Analysis Methods for Submicron Indentation Testing, *Vacuum*, 2000, **58**, p 569-585
9. V.Y. Shevchenko, A.E. Madison, and G.S. Yur'ev, Structure of Nanodiamonds, *Glass Phys. Chem.*, 2006, **32**, p 261-266
10. Y. Gogotsi, T.K. Klaus, G. Nickel, and M.E. Zvanut, Hydrothermal Behavior of Diamond, *Diam. Relat. Mater.*, 1998, **7**, p 1459-1465
11. A.C. Ferrari and J. Robertson, Raman Spectroscopy of Amorphous, Nanostructured, Diamond-like Carbon, and Nanodiamond, *Phil. Trans. R. Soc. Lond. A*, 2004, **362**, p 2477-2512
12. K. Behler, M. Havel, and Y. Gogotsi, New Solvent for Polyamides and its Application to the Electrospinning of Polyamides 11 and 12, *Polymer*, 2007, **48**, p 6617-6621
13. S.G. Advani, *Processing and Properties of Nanocomposites*, World Scientific Publishing, Hackensack, NJ, 2007
14. V.Y. Dolmatov, Detonation Synthesis Ultradispersed Diamonds: Properties and Applications, *Russ. Chem. Rev.*, 2001, **70**(7), p 607-626